LIMNOLOGY
and
OCEANOGRAPHY

ASLO

Limnol. Oceanogr. 9999, 2020, 1–13

doi: 10.1002/lno.11581

Using chlorophyll fluorescence kinetics to determine photosynthesis in aquatic ecosystems

Maxim Y. Gorbunov [1*], **Paul G. Falkowski** [1,2]

[1]Environmental Biology and Molecular Ecology Program, Department of Marine and Coastal Sciences, Rutgers, The State University of New Jersey, New Brunswick, New Jersey

[2]Department of Earth and Planetary Sciences, Rutgers, The State University of New Jersey, Piscataway, New Jersey

Abstract

Variable fluorescence techniques are increasingly used to assess phytoplankton photosynthesis. All fluorescence techniques and models for photosynthetic electron transport rates (ETRs) are amplitude-based and are subject to errors, especially when phytoplankton growth is nutrient-limited. Here we develop a new, kinetic-based approach to measure, directly and in absolute units, ETRs and to estimate growth rates in phytoplankton. We applied this approach to investigate the effects of nitrogen limitation on phytoplankton photophysiology and growth rates. Nutrient stress leads to a decrease in the quantum yield of photochemistry in Photosystem II (F_v/F_m); however, the relationship between F_v/F_m and growth rates is highly nonlinear, which makes it impossible to quantify the reduction in phytoplankton growth rates from F_v/F_m alone. In contrast, the decline in growth rates under nitrogen stress was proportional to the decrease in kinetic-based photosynthetic rates. Our analysis suggests the kinetic fluorescence measurements markedly improve the accuracy of ETR measurements, as compared to classical amplitude-based measurements. Fluorescence-based methods for primary production rely on measurements of ETRs and then conversion to carbon fixation rates by using the electron yields of carbon fixation. The electron yields exhibit 10-fold variability in natural phytoplankton communities and are strongly affected by nutrient limitation. Our results reveal that a decrease in the growth rates and the electron yields of carbon fixation is driven by, and can be quantified from, a decrease in photosynthetic turnover rates. We propose an algorithm to deduce the electron yields of carbon fixation, which greatly improve fluorescence-based measurements of primary production and growth rates.

In contrast to terrestrial ecosystems, oceanic primary production and growth are fundamentally limited by the availability of nutrients, such as nitrogen and iron, and in some regions colimited by phosphorus. The paucity of nutrients in the global ocean leads to a substantial decrease in the efficiency of oceanic photosynthesis. On the global scale, oceanic phytoplankton operates at only ~ 50% of its potential maximum (Lin et al. 2016). At first approximation, the distributions of nutrient stress in the global ocean show a marked meridional pattern, with most of tropical and subtropical gyres being limited by the paucity of nitrogen and polar and subpolar regions by iron (Moore et al. 2013). The physiological effects of nutrient stress on phytoplankton growth are determined by the concentrations and fluxes of nutrients in the upper water column and these fluxes are highly dynamic and variable in space and time. Also, susceptibility to nutrient stress varies significantly among phytoplankton species, taxa, and size groups (Sunda and Huntsman 1997; Litchman and Klausmeier 2008). Understanding and quantifying the effects of nutrient stress on primary production is a fundamental task of biological oceanography and addressing this challenging task requires development of technologies for rapid identification and quantitative analysis of nutrient stress in the ocean.

Chlorophyll *a* (Chl *a*) fluorescence techniques are commonly used to measure biomass and physiological status of phytoplankton and benthic organisms in marine ecosystems (Falkowski et al. 2004). Assessment of the photosynthetic efficiency in these organisms relies on the measurement and analysis of Chl *a* "variable fluorescence," a property unique to the photosynthetic machinery (Falkowski et al. 2004). Variable Chl *a* fluorescence is the most sensitive, nondestructive signal detectable in the upper ocean that reflects instantaneous phytoplankton photophysiology and photosynthetic rates (Falkowski and Kolber 1995; Kolber et al. 1998). Variable fluorescence techniques rely on the relationship between fluorescence yields and the efficiency of photosynthetic processes and provide a comprehensive suite of characteristics of energy transfer in light-harvesting complexes, photochemical reactions in Photosystem

*Correspondence: gorbunov@marine.rutgers.edu

II (PSII) reaction centers, and photosynthetic electron transport down to carbon fixation (Table 1).

Assessment of the impact of nutrient limitation and other stressors on physiology and growth of marine biota is based on measurements of the quantum yield of photochemistry in PSII, or potential photosynthetic efficiency, known as an F_v/F_m ratio. In the case of nitrogen limitation, however, the relationship between F_v/F_m and phytoplankton growth rates is highly nonlinear (Kolber et al. 1988; Parkhill et al. 2001), which makes it impossible to quantify the reduction in phytoplankton growth rates under nutrient stress from F_v/F_m alone. Also, both Fe and N limitation lead to a decrease in F_v/F_m that requires development of additional, stress-specific indicators, or a suite of indicators, suitable for identification and quantification of Fe and N limitation in the ocean.

Variable fluorescence techniques (such as fast repetition rate fluorescence [FRR] or fluorescence induction and relaxation [FIRe]) provide ultra-fast and sensitive tools to derive the light-driven electron flux in PSII, commonly called photosynthetic electron transport rates (ETRs) (Genty et al. 1989, 1990; Kolber and Falkowski 1993). ETRs can then be converted to the rates to carbon fixation using the electron requirements (or electron yields) of carbon fixation (Lawrenz et al. 2013; Hughes et al. 2018*a*). Field observations suggest that this conversion factor exhibits ~ 10-fold variability in natural phytoplankton communities and is strongly affected by the extent of nutrient limitation, taxonomic composition, and other factors (Lawrenz et al. 2013; Schuback et al. 2017; Hughes et al. 2018*b*). Understanding the factors that control the electron requirements of carbon fixation and development of methods to predict this critical variable is important for improving fluorescence-based measurements of primary production.

All modern models to derive ETRs and photosynthetic rates rely on the use of amplitude-based variable fluorescence (Genty et al. 1989; Kolber and Falkowski 1993; Oxborough

Table 1. Notations, abbreviations, and terminology.

	Description	Units
ETR_{Fv}	Electron transport rate from amplitude-based variable fluorescence analysis	e s^{-1} $PSII^{-1}$
ETR_{τ}	Electron transport rate from kinetic fluorescence analysis	e s^{-1} $PSII^{-1}$
PAR	Photosynthetically available radiation	μmol quanta m^{-2} s^{-1}
σ_{PSII}	Functional absorption cross section of photosystem II (PSII)	$Å^2$ or m^2
F_o, F_m	Minimum and maximum yields of Chl *a* fluorescence measured in a dark-adapted state	a.u.
F_v	Variable fluorescence (= $F_m - F_o$)	a.u.
F_v/F_m	Maximum quantum yield of photochemistry in PSII, measured in a dark-adapted state	Dimensionless
p	"Connectivity factor," defining the probability of the excitation energy transfer between individual photosynthetic units	Dimensionless
F_o', F', F_m'	Minimum, steady state, and maximum yields of Chl *a* fluorescence measured under ambient light. F_o' can be measured after a brief (~ 1 s) period of darkness to promote opening of all reaction centers	a.u.
$\Delta F'$	Change in the fluorescence yield measured under ambient light (= $F_m' - F'$)	a.u.
F_v'	Maximum variable fluorescence measured under ambient light (= $F_m' - F_o'$). Here F_o' and F_m' corresponds to fully open and closed reaction centers, respectively.	a.u.
$\Delta F'/F_v'$	Coefficient of photochemical quenching, which is a fraction of open reaction centers in a light-adapted state.	Dimensionless
$\Delta F'/F_m'$	Quantum yield of photochemistry in PSII, measured under ambient light ($\Phi_{PSII} = [F_m' - F']/F_m'$)	Dimensionless
F_v'/F_m'	Quantum efficiency of photochemistry in open reaction centers of PSII, measured in a light-adapted state (= $[F_m' - F_o']/F_m'$)	Dimensionless
PQ	Plastoquinone pool, the pool of electron carriers between PSII and photosystem I (PSI)	Molecules/PSII
PQ_{ox}	The redox state of the PQ pool, normalized to unity. PQ_{ox} varies from 1 (fully oxidized) to 0 (fully reduced).	Dimensionless
$\phi_{e,C}$	Electron requirement for carbon fixation (the number of electrons required to accumulate one C)	e/C
NP_C	Net primary production	μmol C s^{-1}
Φ_{NPc}	Electron yield of net primary production (the number of accumulated C per one electron produced in PSII)	C/e
$1/\tau$	Photosynthetic turnover rate	s^{-1}
τ	Photosynthetic turnover time	s
$\tau_{replete}$	Photosynthetic turnover time for nutrient-replete growth	s
$x = \tau_{replete}/\tau$	Relative decrease in photosynthetic turnover rate by nitrogen stress	Dimensionless

et al. 2012). For instance, the key parameter in these models is a change in the amplitude of Chl *a* fluorescence ($\Delta F'/F_m'$) as a proxy for the quantum yield of photochemistry in PSII under ambient irradiance (Genty et al. 1989). The ETRs are not measured directly; instead they are derived based on a biophysical model of energy conversion in PSII. Is there a better, more direct way to measure photosynthetic rates?

Kinetic analysis is an analytical method for quantitative time-resolved observation of how the concentrations of the reactants in a chemical reaction change over time. Kinetic analysis is the basal approach in chemical kinetics and photochemistry for most accurate measurements of the rate (or rates, if multiple processes are involved) of chemical reactions. This type of analysis can be applied to measure the rates of photosynthetic electron transport by monitoring the kinetics of Q_a reoxidation in PSII (i.e., transition $Q_a^- \rightarrow Q_a$, where Q_a is the first quinone acceptor of PSII) (Crofts and Wraight 1983; Kolber et al. 1998). Because the redox state of this Q_a acceptor affects the optical properties of PSII (such as the quantum yield of fluorescence), the kinetics of Q_a reoxidation can be directly derived from the relaxation kinetics of Chl *a* fluorescence yield after a saturating flash of light, which fully reduces Q_a (Kolber et al. 1998). Several operational instruments, including FRR and FIRe fluorometers, have been developed for this kind of kinetic analysis, but application of these instruments for kinetic analysis of photosynthetic rates remained unexplored.

The objectives of this work are: (1) to examine the capabilities of fluorescence kinetic analysis for measurements of photosynthetic ETRs and rates of primary production; (2) to investigate the effect of nitrogen stress on kinetic characteristics and photosynthetic rates in model phytoplankton species, with the overarching goal to improve fluorescence-based measurements of primary production and growth rates; and (3) to develop operational, ultra-sensitive fluorescence instruments that combine amplitude-based and kinetic analysis of fluorescence yields and photosynthetic rates.

This research is aimed at testing the following hypotheses: (1) Photosynthetic rates and growth rates in phytoplankton are controlled by the rate of photosynthetic electron flow and this rate can be accurately determined from the kinetic measurements of Chl *a* fluorescence relaxation kinetics; (2) direct, kinetic measurements of photosynthetic ETRs are more accurate than classical amplitude-based measurements; (3) the combination of amplitude-based and kinetic analyses provides quantitative, stress-specific diagnostics of nutrient stress in oceanic ecosystems and allows one to improve fluorescence-based measurements of primary production.

Methods and materials

Mini-FIRe fluorometers and measurement protocols

Variable fluorescence and photosynthetic characteristics were measured with new miniaturized Fluorescence Induction and Relaxation Systems (called mini-FIRe) (Fig. 1). These instruments are conceptually similar to previous FRR (Kolber et al. 1998) and FIRe systems (Gorbunov and Falkowski 2005), but exhibit approximately 20-fold higher sensitivity and signal-to-noise ratio, compared to their predecessors. This extreme sensitivity is crucial for sampling in oligotrophic regions, which constitute 30% of the world ocean (Lin et al. 2016). High signal-to-noise ratio is crucial for precise analysis of fluorescence relaxation kinetics (Gorbunov et al. 1999).

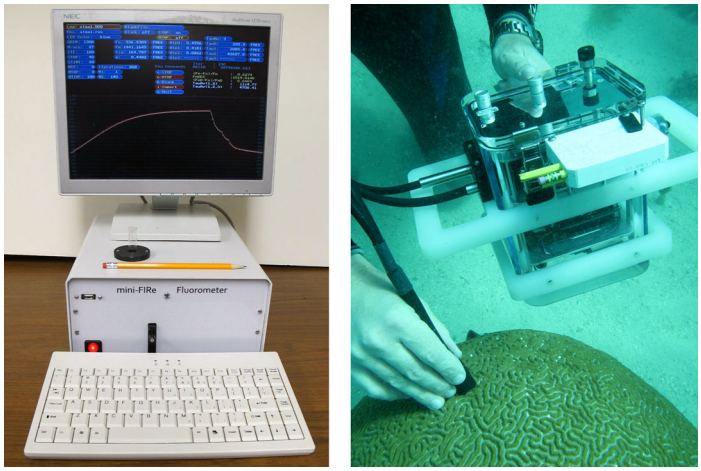

Fig. 1. (Left) Benchtop fluorescence induction and relaxation instrument (a mini-FIRe); (Right) Diver-operated FIRe system for in situ measurements of photosynthetic characteristics and photosynthetic rates on benthic organisms, such as coral, marcophytes, and seagrasses.

We developed and manufactured several versions of mini-FIRe fluorometers. These include a basic low-cost benchtop version that employs excitation at a single wavelength (450 nm, with a half-bandwidth of 20 nm) and a multicolor mini-FIRe instrument (Gorbunov et al. 2020) with excitation at multiple wavelengths (435, 450, 470, 500, 530, and 590 nm, with 20 nm half bandwidth for each channel). This multicolor excitation allows for selective excitation of different functional groups of phytoplankton, as well as for spectrally resolved measurements of functional absorption cross-sections of PSII. This multicolor instrument is designed to monitor both physiological characteristics and changes in taxonomic composition of phytoplankton communities (Gorbunov et al. 2020). Finally, a diver-operated underwater mini-FIRe fluorometer (Fig. 1) is designed for in situ sampling on benthic organisms, including coral or macroalgae.

The peak excitation intensity in the measuring volume of the FIRe instrument is optimally adjusted to ensure closure of PSII reaction centers and saturation of fluorescence within approximately 100 μs (i.e., a single electron turnover in PSII) (Gorbunov et al. 2020), which is crucially important for accurate retrievals of functional cross sections and quantum yields (Gorbunov et al. 1999). The fluorescence signal is collected

from a central, 8 mm diameter, portion of the sample volume, isolated by a red band pass interference filter (680 nm, with 20 nm bandwidth), and detected by an avalanche photodiode (SD630-70-72-500, Advanced Photonics). The replaceable emission filter permits measurements of fluorescence signals from different fluorescent pigments, such as Chl *a*, phycobilins, or bacteriochlorophyll. The voltage on the detector is automatically adjusted, depending on ambient temperature, to ensure a constant gain over a wide temperature range (0 to 30°C). By using an avalanche photodiode with high quantum efficiency in the red spectral region (ca. 80%) and integrating the fluorescence signal in the analog mode, the instrument operates with an extremely high signal-to-noise ratio. The mini-FIRe instrument can accurately measure fluorescence signals in samples as low as 0.01 mg chlorophyll m^{-3}—effectively the lowest concentration of chlorophyll recorded anywhere in the upper ocean.

To record fluorescence signals under ambient light, including light curves (i.e., photosynthesis vs. irradiance, or P vs. E), the FIRe fluorometer incorporates an actinic light source that is controlled by the FIRe computer. This light source provides uniform illumination of the entire volume of the sample cuvette, which is critical for accurate recording of slow P vs. E curves. The P vs. E curves can be recorded, in a fully automatic mode, on discrete samples or during underway continuous sampling at sea in a stop-flow regime.

The photosynthetic turnover time

The photosynthetic turnover time (τ) is defined as the time required for the products of primary photochemical reactions (i.e., electrons produced as a result of charge separation in reaction centers) to complete the whole cycle of transfer from reaction centers to ribulose-1,5-bisphosphate carboxylase/oxygenase (RUBISCO) and CO_2 fixation (Herron and Mauzerall 1971; Myers and Graham 1971). The reciprocal of the turnover time ($1/t$) is the turnover rate, which determines the maximum rate of this process (P^{max}).

Functional absorption cross-sections

The functional absorption cross-section of PSII (σ_{PSII}) is a product of the optical absorption cross-section of PSII (i.e., the physical size of the PSII antennae) and the quantum yield of photochemistry in PSII (Falkowski et al. 2004). σ_{PSII} is calculated from the rate of fluorescence rise during the single turnover flash (Kolber et al. 1998). This rate is proportional to the product of σ_{PSII} and the photon flux density of excitation light (Gorbunov and Falkowski 2005). Retrievals of σ_{PSII} in absolute units ($Å^2$) require accurate calibration of the average photon flux density in the measuring volume, that is, the volume from which the signal is recorded (Gorbunov and Falkowski 2005). Because amplitude-based measurements of absolute ETR depend on σ_{PSII}, accurate calibration of excitation intensities is crucially important.

Analysis of fluorescence relaxation kinetics

The kinetics of electron transport on the acceptor side of PSII (i.e., Q_a oxidation) is assessed from analysis of the relaxation kinetics of fluorescence yield following a saturating single turnover flash (Kolber et al. 1998; Gorbunov and Falkowski 2005). These kinetics consist of several components because the rate of Q_a reoxidation depends on the state of the second quinone acceptor, Q_b, which is a mobile two-electron acceptor (Crofts and Wraight 1983):

$$Q_a^- \, Q_b \rightarrow Q_a \, Q_b^- \; (150 - 200 \mu s) \tag{1}$$

$$Q_a^- \, Q_b^- \rightarrow Q_a \, Q_b^{=} \; (600 - 800 \mu s) \tag{2}$$

$$Q_a^- \rightarrow Q_a^- \, Q_b \rightarrow Q_a \, Q_b^- \; (\sim 2000 \mu s) \tag{3}$$

Reaction (3) corresponds to the conditions when the Q_b is initially out of its binding site on the D1 protein. Also, a fraction of inactive reaction centers with impaired electron transport may contribute to the slowest component (τ_3) in the relaxation kinetics. Here, we analyzed the relaxation kinetics using a three-component analysis and calculated the average time constant (reported below as τ_{Qa}) for the two fastest components (τ_1 and τ_2):

$$\tau_{Qa} = (\alpha_1 \, \tau_1 + \alpha_2 \, \tau_2) / (\alpha_1 + \alpha_2)$$

Thus, this average time constant, τ_{Qa}, reflects the rate of Q_a reoxidation in active reaction centers.

Amplitude-based fluorescence measurements of ETR

Absolute ETR per open PSII reaction center is calculated from the product of light intensity (E), the optical absorption cross-section of PSII, σ_{PSII}^{opt} (i.e, how much light is absorbed by a PSII unit), and the quantum yield of photochemistry in PSII, Φ_{PSII} (i.e., the portion of absorbed photons that produce electron flow in PSII). This product must be further multiplied by a fraction of dynamically open centers ($\Delta F'/F_v'$) to reflect the fact that a fraction of reaction centers become dynamically closed under ambient light and only the remaining open centers contribute to photosynthetic energy utilization (Falkowski et al. 1986). The fraction of open reaction centers (also called the coefficient of photochemical quenching) can be measured by variable fluorescence technique as a ratio of variable fluorescence under a given irradiance ($\Delta F'$) to the maximum variable fluorescence (F_v') for this irradiance level. F_v' can be measured after a brief ($\sim$ 1 s) period of darkness to promote opening of all reaction centers that were dynamically closed by ambient light. Therefore, ETR, as a function of irradiance, is expressed as follows:

$$ETR_{Fv} = E \, \sigma_{PSII}^{opt} \, \Phi_{PSII} \, (\Delta F' / F_v') \tag{4}$$

The product of the optical absorption cross-section and the quantum yield of photochemistry in PSII is defined as the

functional absorption cross section of PSII ($\sigma_{PSII} = \sigma_{PSII}^{opt}\ \Phi_{PSII}$) and this parameter is directly measured using the FRR/FIRe technique. Therefore, Eq. 4 can be modified as follows (Gorbunov et al. 2000, 2001):

$$ETR_{Fv} = E\,\sigma_{PSII}'\,(\Delta F'/F_v') \quad (5)$$

Here, σ_{PSII}' is the functional absorption cross section of PSII and $\Delta F'/F_v'$ is the coefficient of photochemical quenching, recorded at a given level of ambient irradiance. By definition, $\Delta F'/F_v' = 1$ in the dark and decreases with irradiance as more reaction centers become dynamically closed by ambient light. The prime character indicates the measurements under ambient irradiance. Both σ_{PSII}' and $\Delta F'/F_v'$ are a function of irradiance.

When nonphotochemical quenching is caused by thermal dissipation in the light-harvesting antennae, Eq. 5 can be reduced to the following (Gorbunov et al. 2000):

$$ETR_{Fv} = E\,\sigma_{PSII}\,[(\Delta F'/F_m')/(F_v/F_m)] \quad (6)$$

where $\Delta F'/F_m'$ is the actual quantum yield of photochemistry in PSII at a given irradiance level. $\Delta F'/F_m'$ is an irradiance-dependent parameter in Eq. 6 and can be directly measured by FRR/FIRe techniques. It should be noted that the use of Eq. 5 requires measurements under both ambient light and after a brief period darkness (e.g., in both open and dark chambers of the in situ FRR fluorometer). For instance, $F_v' = F_m' - F_o'$ can be only recorded after a brief (~ 1 s) period of darkness, which is required for all reaction centers to open and for fluorescence yield to reach F_o' level. In contrast, Eq. 6 includes parameters recorded only under ambient light, thus eliminating the need to make measurements in darkness.

Kinetic-based measurements of ETR

Kinetic measurements of the absolute ETR rely on the rate of photosynthetic turnover ($1/\tau$), which defines maximum ETR achieved under saturating irradiance. The shape of ETR(E) in relative units is reconstructed from the dependence of the quantum yield of photochemistry in PSII ($\Delta F'/F_m'$ as a function of E):

$$ETR_\tau = 1/\tau\,(E\,\Delta F'/F_m')/(E_{max}\,\Delta F'/F_m'(E_{max})) \quad (7)$$

Here, the relative ETR(E) = $E\ \Delta F'/F_m'$ is normalized to unity by division to its maximum value $E_{max}\ \Delta F'/F_m'(E_{max})$, which is recorded at saturating irradiance (E_{max}). The optimal level of E_{max} is selected at $E_{max} \sim 3 \times E_k$, where E_k is the light saturating parameter of the P vs. E curve (Falkowski and Raven 2014), to achieve the maximum precision of ETR_τ measurements. Multiplication of the relative ETR by the photosynthetic turnover rate ($1/\tau$) provides the absolute ETR_τ per PSII unit. $1/\tau$ is calculated directly from the FIRe determined relaxation at saturating irradiance, using the kinetic analysis (*see* Fig. 2B).

Measurements of the redox state of the PQ pool

The redox state of the PQ pool and its alterations with ambient irradiance were assessed from the analysis of fluorescence induction curves on the millisecond time scale in response to a saturating multiple turnover flash of 200 ms duration. To take into account irradiance-induced effects of nonphotochemical quenching of chlorophyll fluorescence, the variable component (F_v) of the induction curve was normalized to unity at each irradiance light level. The fraction of the oxidized PQ molecules (noted as PQ_{ox}) as a function of ambient irradiance was estimated from a reduction in the area above the normalized induction curve relative to the reference area measured for fully oxidized PQ pool (Falkowski and Raven 2014; Levitan et al. 2015). This reference area is calculated from the induction curve recorded after a short (1 s) period of darkness followed by a short (1 s) pre-exposure to far-red light (the wavelengths > 700 nm).

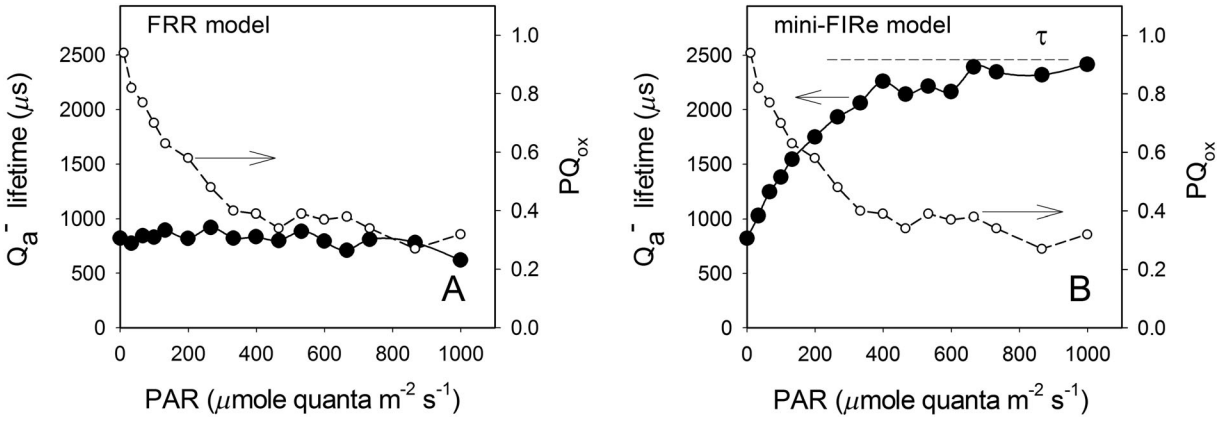

Fig. 2. The effect of ambient PAR on the time of Q_a reoxidation (solid dots), in relation to PAR-driven alterations in the redox state of the PQ pool (PQ_{ox}, open dots). These time constants were retrieved from the kinetics of fluorescence relaxation in the diatom, *T. pseudonana*, following a saturating single turnover flash by using two different mathematical models, the FRR model (**A**) and the new mini-FIRe model (**B**).

Strains and culture conditions

Algal cultures were grown at 18°C in F/2 medium under continuous white light (500 μmol photons m^{-2} s^{-1}) from light-emitting diode lamps. This high irradiance was chosen to ensure that photosynthetic rates were at their maximum level (P^{max}) and the growth was maximal. These cultures included diatoms (*Thalassiosira pseudonana* CCMP1335, *Thalassiosira weissflogii* CCMP1336, *Thalassiosira oceanica* CCMP1005, *Phaeodactylum tricornutum* CCMP632), and a chlorophyte (*Dunaliella tertiolecta* CCMP1320).

Nutrient stress experiments

Nutrient stress experiments were conducted on batch cultures growing in low-nitrogen media. First, cultures were preacclimated (for 4–5 d) to low-nitrogen F/2 media, with [NO_3] of 10 μmol L^{-1}, which is 90 times lower than in normal. This preacclimation allowed the cells to maintain maximum growth rates even in this low-nitrogen media, although the cellular Chl *a* content reduced several fold, a sign of acclimation to low-nitrogen conditions (Parkhill et al. 2001). Then we monitored, in batch cultures, the slowly progressing nutrient stress, as the cells digested the remaining [NO_3] and the nitrogen concentration in the media became undetectable within 48–72 h. The Chl *a* concentration in the samples during these experiments did not exceed 5–10 mg Chl m^3.

Growth rates measurements

Instantaneous growth rates (μ) were determined from an increase in cell density (N, cell mL^{-1}) over a short (4–6 h) period of time (Δt), using an exponential growth equation:

$$\mu = \ln[N(t+\Delta t)/N(t)]/\Delta t \quad (8)$$

Cell densities were recorded using Beckman Coulter Multisizer 3 cell counter.

Mathematical formalism for fluorescence relaxation kinetics

The induction of fluorescence yield during a saturating single-turnover flash is driven by accumulation of closed reaction centers $C(t)$ over time and the resulting increase in fluorescence yield $F(t)$ from its minimum (F_o) to maximum (F_m) values (Table 1). The rate of increase in $C(t)$ is driven by the rate of photochemical charge separation in PSII reaction centers and determined by σ_{PSII}, the photon flux density (I), and the extent of energy transfer between reaction centers (called "connectivity factor," p):

$$dC(t)/dt = \sigma_{PSII} I\,(1-C(t))/(1-pC(t)) \quad (9)$$

$$F(t) = F_o + F_v\,C(t)\,(1-C(t))/(1-pC(t)) \quad (10)$$

Here, $F_v = F_m - F_o$ is the variable fluorescence yield. These equations assume that the rate of photochemistry in PSII induced by the saturating single turnover flash is much faster than the rate of Q_a^- reoxidation and the latter can be ignored. In the general case (e.g., when the rate of fluorescence induction is comparable to the rate of Q_a^- reoxidation), the Q_a^- reoxidation kinetics can be taken into account, at the expense of more complex mathematical formalism, as described below.

The relaxation kinetics of fluorescence yield after a saturating single turnover flash is driven by the kinetics of Q_a^- reoxidation and the resulting conversion of RCs back to the open state. However, the measured kinetics is also affected by the rate of photochemistry produced by measuring flashes and by actinic (ambient) light. These two processes slow down reopening of reaction centers and thus distort the measured fluorescence relaxation kinetics. These must be taken into account while retrieving the actual kinetic rates of Q_a^- reoxidation. Below we explain, in turn, why and how these two processes must be incorporated into mathematical formalism.

Kinetics of Q_a^- reoxidation are recorded by applying a sequence of relatively weak relaxation flashlets followed at progressively increasing intervals between these flashlets (Gorbunov and Falkowski 2005). Under such conditions, the observed kinetics of $C(t)$ relaxation between the flashlets is driven by two competing processes: Q_a reoxidation and the actinic effect of ambient light. The former leads to conversion of reaction centers to the open state, while the latter returns a fraction of centers back to the closed state. A change in $C(t)$ between the flashlets is described as follows:

$$C(t_i+\Delta T) = C(t_i)\,\{\alpha_1 \exp(-\Delta T/\tau_1) + \alpha_2 \exp(-\Delta T/\tau_2) + \alpha_3 \exp(-\Delta T/\tau_3)\} + \sigma_{PSII}\,PAR\,\Delta T\,(1-C(t_i))/(1-C(t_i)p) \quad (11)$$

Here, ΔT is the interval between relaxation flashes, τ_1, τ_2, and τ_3 are the time constants fast, medium, and slow components of Q_a reoxidation, α_1, α_2, and α_3 are relative magnitudes of these components ($\alpha_1 + \alpha_2 + \alpha_3 = 1$), and PAR is the intensity of ambient light, or photosynthetically available radiation. Equation 11 assumes that the kinetics of Q_a reoxidation is multicomponent. Our analysis revealed that at least three components are usually needed to describe these kinetics with sufficient accuracy. The interval between relaxation flashes is assumed to be short ($\Delta T << [\sigma_{PSII}\,PAR]^{-1}$). The first term in the Eq. 11 describes opening the reaction centers due to Q_a reoxidation, while the second term—partial conversion of reaction centers back to the closed state due to the photochemistry induced by ambient light. The incorporation of PAR in Eq. 11 is crucially important for accurate retrievals of the rates of Q_a reoxidation measured under ambient light.

If the intensity of relaxation measuring flashes would be negligible, the measured relaxation kinetics in darkness would precisely follow the kinetics of Q_a^- reoxidation. However, the induced fluorescence signals would be extremely weak and noisy. To achieve a suitable signal-to-noise, the intensity of measuring flashlet is set at approximately 0.02 μmol quanta m^{-2}

per flash with 1 μs duration, which corresponds to approximately 0.05 hits per reaction center per flash. This number is not negligible; each flashlet produces a small, but significant, increase in the fraction of closed reaction centers. This increase in $C(t)$ by the measuring relaxation flashlet is numerically described as follows:

$$\Delta C = \sigma_{PSII} I \Delta t_{relax} (1 - C(t))/(1 - pC(t)) \quad (12)$$

where Δt_{relax} is the duration of the relaxation flashlet (1 μs in FIRe instruments), I is the peak intensity of measuring excitation light, and $C(t)$ is the fraction of closed centers at the beginning of the relaxation flashlet. The measured FIRe relaxation kinetics is processed by numerically fitting these profiles to Eqs. 9–12 to retrieve correct time constants (τ_1, τ_2, τ_3) of Q_a reoxidation kinetics.

Results

Variable fluorescence in a dark adapted state provides the maximum quantum yield of photochemistry in PSII (F_v/F_m), which reflects the potential photosynthetic efficiency. This parameter is the most commonly used indicator of photosynthetic competence and environmental stresses (Falkowski et al. 2004), but alone it does not reflect the actual photosynthetic rates achieved under ambient irradiance. Variable fluorescence signals must be recorded in a light-acclimated state to infer the actual photosynthetic rates and to estimate the rates of primary production (e.g., Genty et al. 1989; Kolber and Falkowski 1993). Amplitude-based variable fluorescence signals as a function of irradiance provide a conceptual framework for retrieving instantaneous photosynthetic rates (called photosynthesis vs. irradiance, or P vs. E curves). We examined how kinetic variable fluorescence measurements can be used to infer the actual rates of photosynthetic electron transport and how kinetic analysis can improve measurements of photosynthetic rates.

Effect of ambient irradiance on the kinetics of electron transport in PSII

We first employed the standard FRR model and measurement protocol (Kolber et al. 1998) to examine how the observed fluorescence relaxation kinetics changes with irradiance. We expected that as PAR increases and the PQ pool becomes reduced, the actual rate of electron flow would slow down and the rates of FRR fluorescence relaxation kinetics would decrease. Unexpectedly, we found that the FRR retrieved relaxation rates remained virtually unchanged with an increase in PAR, even when the PQ pool became reduced at saturating PAR (Fig. 2A). Such pattern was observed in all algal species and samples of natural phytoplankton we analyzed. Why does not the FRR relaxation analysis show a decrease in the speed of electron flow under saturating irradiances?

The FRR model was originally developed for analysis of fluorescence transients in dark-adapted samples (Kolber et al. 1998). This model and mathematical framework did not include the effects of ambient irradiance on the measured fluorescence relaxation kinetic. As ambient light promotes dynamic closure of a fraction of reaction centers, this process competes with Q_a reoxidation and inevitably distorts the observed Q_a reoxidation kinetics.

To overcome this limitation of the FRR technique, we developed a new mathematical model and numerical fitting procedure for kinetic data analysis (*see* "Methods and Materials" section). This procedure has been implemented in the new mini-FIRe instruments. We employed this new approach to calculate the rates of Q_a reoxidation measured under ambient irradiance and examined how these rates changes with PAR (Fig. 2B**)**. This new analysis revealed a strong affect of irradiance on the rates and time constants (τ_{Qa}) of Q_a reoxidation. In darkness or under low PAR, the PQ pool is oxidized (i.e., PQ_{ox} = 1), τ_{Qa} is fast. As PAR increases, the PQ pool becomes more reduced and, consequently, τ_{Qa} increases, reflecting a decrease in the speed of electron flow (Fig. 2B).

At saturating irradiance, τ_{Qa} plateaus, closely approaching the photosynthetic turnover time (Fig. 2B). This data suggest that under saturating irradiance, the maximum flux of electrons is determined and limited by the speed at which the electrons can move through the electron transport chain. This result has an important implication as our new kinetic protocol offers a simple practical way to measure photosynthetic turnover rates from fluorescence relaxation kinetics recorded under saturating PAR.

Effect of nitrogen limitation on the kinetics of photosynthetic electron transport

Phytoplankton photosynthesis in the global ocean is fundamentally limited by the availability of nutrients, such as nitrogen and iron (Lin et al. 2016). How does nutrient limitation affect the kinetic properties of photosynthetic electron transport? Can kinetic analysis tell us about the impact of nutrient limitation on primary production and phytoplankton growth rates in the global ocean? How can the new kinetic-based analysis improve the capabilities of Chl *a* variable fluorescence for quantitative assessment of nutrient stress in the ocean?

To address these questions, we examined the effects of nitrogen stress on the kinetic parameters of photosynthetic electron transport in two model species: the diatom, *Thalassiosira pseudonana*, and the chlorophyte, *Dunaliella tertiolecta*. We quantified the extent of nitrogen limitation from the reduction in the quantum yield of photochemistry in PSII (F_v/F_m) and growth rates. Figure 3 shows the effect of nitrogen limitation on the kinetic characteristics of Q_a reoxidation in the marine diatom *T. pseudonana*. This profile (open dots) was recorded when growth rate was dramatically reduced by N stress (0.2 d^{-1}, as compared to 1.5 d^{-1} in the

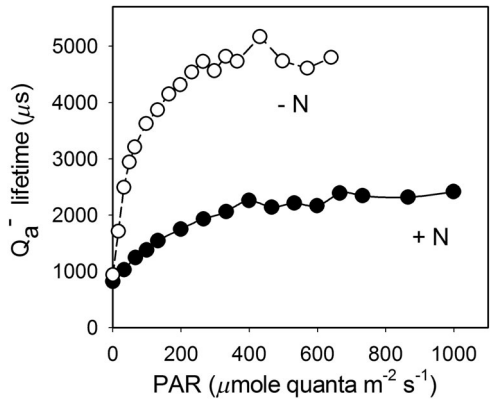

Fig. 3. Effect of nitrogen limitation on kinetics of electron transport in PSII (Q_a reoxidation) as a function of PAR. The profiles τ_{Qa}(PAR) were recorded in the diatom, *T. pseudonana*, under nutrient-replete (+N) and nitrogen-limited (–N) conditions.

nutrient-replete control, solid dots). In spite of dramatic reduction in the growth rate, the F_v/F_m ratio remained high (0.48 vs. 0.6 in the nutrient-replete control). Similar patterns were observed in other phytoplankton model species (*T. thalassiosira*, *P. ticornutum*, *T. oceanica*, *D. tertiolecta*) and natural samples of N-stressed phytoplankton. This analysis revealed that the time constant for Q_a reoxidation (τ_{Qa}) in darkness was not affected by N stress (Fig. 3), suggesting that the kinetics of Q_a reoxidation in a dark adapted state is not an indicator of N stress. In contrast, τ_{Qa} recorded under saturating light increased dramatically under N limitation (Fig. 3). This increase reflects an increase in the photosynthetic turnover time and the resulting reduction in the maximum rates of electron transport.

Revaluating the relationship between phytoplankton photophysiology and growth rates—The case of nitrogen limitation

Nitrogen limits primary productivity in the most of the global ocean (Dugdale 1967; Eppley 1980; McElroy 1983). To develop a more robust, quantitative diagnostic of nitrogen stress, we examined how nitrogen limitation affects the suite of variable fluorescence characteristics and photosynthetic rates in two model algae, the green alga *D. tertiolecta* (Fig. 4) and the diatom *T. pseudonana* (Fig. 5). The extent of nitrogen stress was quantified from a reduction in instantaneous growth rates.

The relationship between F_v/F_m and growth rates was highly nonlinear, thereby a detectable reduction in F_v/F_m was observed only under severe N stress, when the growth rates were markedly (> 50%) reduced (Fig. 4A). In contrast, the maximum photosynthetic rates P^{max} recorded under high light showed a detectable decrease even at moderate nitrogen stress (Fig. 4B,C).

We further examined two protocols for calculating ETR. The first, classical amplitude-based protocol (ETR_{Fv}) is based on the use of a change in fluorescence yield under a saturating flash, $\Delta F'/F_m'$ as a proxy of the actual quantum yield of photochemistry in PSII under a given level of PAR (*see* Eq. 5). The second, kinetic-based approach (ETR_τ) relies on the kinetic analysis of electron transfer in PSII, which is deduced from fluorescence relaxation kinetics (Fig. 3). Amplitude-based ETR_{Fv} tend to decrease as the growth rates decreased due to nitrogen stress (Figs. 4B, 5B). However, the wide scatter of experimental data points and, as a consequence, the weak correlation between ETR_{Fv} and growth rates did not allow for this dependence to be quantified. In contrast, the correlation between kinetic-based ETR_τ and growth rates was markedly better (Figs. 4C, 5C). Also, the dependence between ETR_τ and growth rates was clearly linear (Figs. 4C, 5C). In *D. tertiolecta*, the regression coefficient between ETR and growth rates was only $R^2 = 0.65$ for amplitude-based ETR_{Fv} and $R^2 = 0.95$ for the kinetic-based ETR_τ (Fig. 4B,C). In *T. pseudonana*, $R^2 = 0.23$ for ETR_{Fv} and $R^2 = 0.76$ for ETR_τ (Fig. 5B,C). These results clearly suggest that the kinetic-based approach dramatically improves the accuracy of ETR measurements and offers a more accurate proxy for the actual photosynthetic rates.

Modeling the effects of nitrogen limitation on growth rates and rates of net primary production

The rate of net primary production is defined by the product of carbon biomass (C) and growth rate (μ):

$$NP_C = dC/dt = C\mu \quad (13)$$

As cell growth drives the rates of net primary production, the relationship between kinetic-based ETR measurements and growth rates (Figs. 4C, 5C) offers a path toward modeling the rates of net primary production from variable fluorescence. How can this relationship be used to convert kinetic-based ETR measurements to the rates of primary production?

Conversion of ETR rates to the rates of carbon fixation relies on the electron requirement of carbon fixation ($\phi_{e,C}$), which is defined as a number of electrons produced in PSII photochemistry required to accumulate one cellular C (Kolber and Falkowski 1993; Lawrenz et al. 2013). By definition, the reciprocal of the electron requirement defines the electron yield of carbon fixation. Here, we define the electron yield of net primary production (Φ_{NPc}) as the ratio of the number of accumulated cellular C to the number of electrons produced by photochemistry in PSII. Φ_{NPc} is the key parameter required for conversion of ETR to the rates of primary production. The observed relationship between ETR and growth rates (Figs. 4C, 5C) clearly suggests that nitrogen limitation imposes a major control on Φ_{NPc}. Indeed, Φ_{NPc} is maximal under nutrient-replete growth and decreases to zero under severe nutrient limitation when the growth rates are impaired.

Our results (Figs. 4C, 5C) revealed a linear relationship between kinetic-based ETR and instantaneous growth rates for conditions when growth is limited by nitrogen. Because the

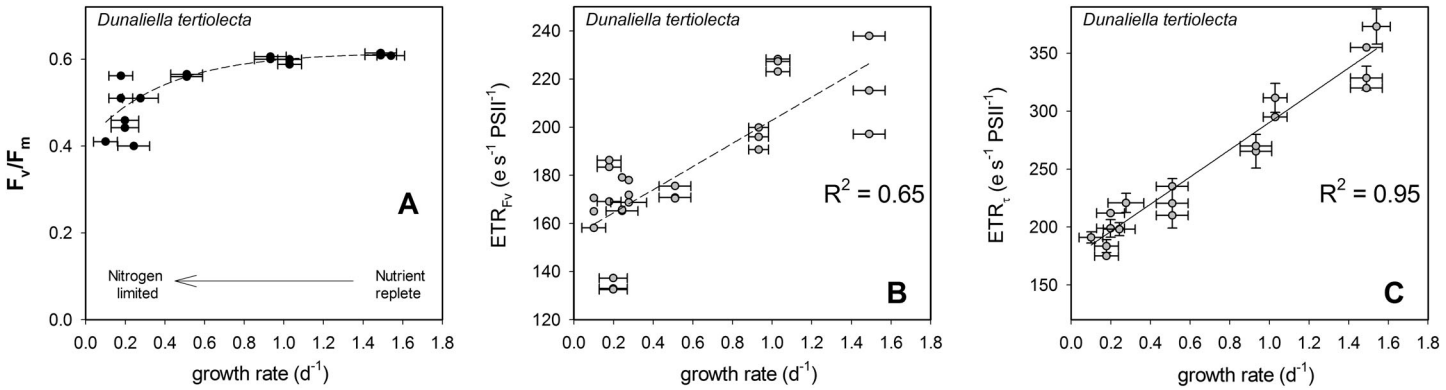

Fig. 4. Effect of nitrogen limitation on photosynthetic characteristics in the green alga, *D. tertiolecta*, in relation to growth rates. (**a**) The quantum yield of photochemistry in PSII, F_v/F_m; (**B**) ETRs deduced from amplitude-based variable fluorescence; (**C**) ETRs deduced from kinetic fluorescence analysis.

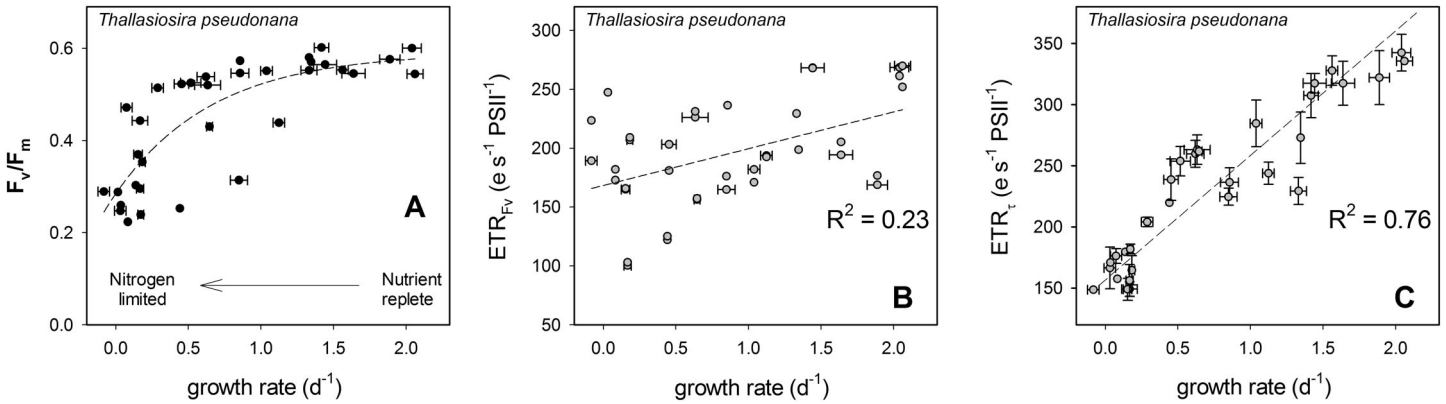

Fig. 5. Effect of nitrogen limitation on photosynthetic characteristics in the diatom, *T. pseudonana*, in relation to growth rates. (**A**) The quantum yield of photochemistry in PSII, F_v/F_m; (**B**) ETRs deduced from amplitude-based variable fluorescence; (**C**) ETRs deduced from kinetic fluorescence analysis.

rate of net primary production is directly proportional to the growth rate (Eq. 13), this linear relationship can be generalized to NP_C as a function of ETR_τ or turnover rates:

$$NP_C = ax - b \tag{14}$$

where $x = \tau_{replete}/\tau$ is the ratio of the turnover rate for a given condition to its maximum value under nutrient-replete conditions. In essence, x is the ratio of ETR_τ to its value under nutrient-replete conditions. The x ratio characterizes the relative reduction in photosynthetic turnover rates by nitrogen limitation.

The electron yield for net primary production (Φ_{NPc}) is, by definition, proportional to the ratio of NP_C to ETR. Therefore, Φ_{NPc} can be expressed as following:

$$\Phi_{NPc} \sim (ax - b)/x \tag{15}$$

This equation for Φ_{NPc} can be scaled to absolute numbers by using experimental values for the electron yields for gross and net primary production for nitrogen-replete growth in diatoms and green algae. Assuming that the electron yield of gross oxygen production (i.e., the number of O_2 molecules evolved per one electron) is 0.25 (Kolber and Falkowski 1993) and the gross-to-net production ratio is 3.3 (i.e., 30% of gross oxygen production is retained as net carbon production) (Halsey et al. 2013, 2014; Juranek and Quay 2013), the maximum electron yield of net carbon production is 0.076. By using this value and fitting our experimental dependence for growth rates as a function of x, we obtained the following dependence for Φ_{NPc}:

$$\Phi_{NPc} = \Phi_{NPc}^{max}\,(1.78x - 0.78)/x \tag{16}$$

where $\Phi_{NPc}^{max} = 0.076$ is the maximum electron yield of net carbon production for nutrient-replete growth and $x = \tau_{replete}/\tau$. The analysis of our experimental data for the diatom, *T. pseudonana*, and the green alga, *D. tertiolecta*, revealed the dependence $\Phi_{NPc}(x)$ was not significantly different ($p > 0.1$) between these two model species (Fig. 6), implying that this relationship might be general for phytoplankton, at least in areas where nitrogen availability limits growth rates.

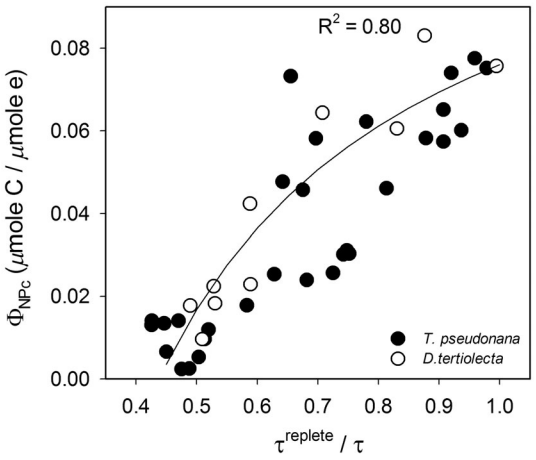

Fig. 6. Effect of nitrogen limitation on the electron yield of net primary production (Φ_{NPc}), in relation to photosynthetic turnover rates ($1/\tau$). The plot combines data for two model phytoplankton species, including the diatom, *T. pseudonana*, and the green alga, *D. tertiolecta*. The turnover rates were calculated from the analysis of FIRe relaxation kinetics under saturating irradiance. τ and $\tau^{replete}$ are turnover times recorded in nitrogen-limited and nitrogen-replete samples, respectively. The ratio of $\tau^{replete}/\tau$ characterizes the relative decrease in photosynthetic turnover rates under nitrogen limitation.

The relative reduction in turnover rates (i.e., the x ratio) can also be used to quantify the reduction in growth rates under nitrogen stress:

$$\mu/\mu^{replete} = 1.85x - 0.85 \quad (17)$$

Here, μ is the actual growth rate, $\mu^{replete}$ is the maximum growth rate under nutrient replete conditions, and $x = \tau_{replete}/\tau$.

We have quantified the relationship between variable fluorescence kinetics and growth rates for nitrogen-limited growth under saturating light. These results have implications for photosynthesis in the upper, well-lit water column of the ocean. The alterations in the growth rates reflect changes in net carbon fixation (Eq. 13). When phytoplankton grow under subsaturating light, the maximum ETR_τ can be scaled down, using the irradiance dependence $ERT_\tau(E)$. However, in this case, net carbon fixation rates will be overestimated, because variable fluorescence does not measure respiration.

Discussion

Fluorescence-based methods for primary production rely on measurements of ETRs in PSII and conversion of these rates to carbon fixation by using the electron requirements of carbon fixation (Kolber and Falkowski 1993; Lawrenz et al. 2013). Field observations suggest that this conversion factor exhibits ~ 10-fold variability in natural phytoplankton communities and is strongly affected by the extent of nutrient, including nitrogen, limitation (Zhu et al. 2017; Hughes et al. 2018*b*; Ko et al. 2019). The accuracy of primary production estimates from variable fluorescence is determined by the two key factors—the accuracy of ETR measurements and that of conversion from ETR to C fixation. Our results revealed that the use of kinetic-based fluorescence analysis markedly improves the accuracy of ETR measurements and allows one to quantify the impact of nitrogen limitation on the electron requirements of carbon fixation, thus improving fluorescence-based estimates of net carbon fixation and growth rates of phytoplankton.

Improving the accuracy of ETR measurements

Amplitude-based variable fluorescence techniques became a workhorse in plant physiology and oceanography to derive ETR in phytoplankton and terrestrial plants (Genty et al. 1989; Kolber and Falkowski 1993; Hughes et al. 2018*a*). Obviously, these techniques do not measure ETR directly; instead ETR are derived from biophysical models. Several models and modifications have been developed (Kolber and Falkowski 1993; Oxborough et al. 2012; Hughes et al. 2018*a*). All these models rely on the use of multiple parameters, such as quantum yield of photochemistry in PSII, effective absorption cross-section of PSII or absorption properties, the amount of open and active reaction centers, spectral incident irradiance including its penetration and attenuation within algal cells or leaves. As a consequence, errors in all parameters add up and inevitably increase the overall error of ETR calculations. Also, some of the model parameters, such as absorption cross-sections and light intensities, critically depend on the accuracy of the instrument calibration. Finally, as amplitude-based ETR rates are not measured directly, the overall accuracy of ETR estimates is further reduced by the model assumptions.

In contrast to amplitude-based fluorescence models for ETR, the kinetic analysis offers a direct way to measure the rates of photochemical reactions in PSII and that of electron transport, thus alleviating caveats of amplitude-based methods. The dramatic improvement in the accuracy of ETR measurements by the kinetic analysis was clearly evident from better correlation between ETR and growth rates (Figs. 4C vs. 4B, 5C vs. 5B). The accuracy of our proposed kinetic-based method is essentially determined by uncertainties of a single variable—the photosynthetic turnover rate (Eq. 7), which markedly improves the accuracy of ETR measurements. The extremely high sensitivity of the developed mini-FIRe instruments allows for this kinetic parameter to be measured at high precision (< 10%) even in oligotrophic waters of the open ocean.

Estimating the electron yield of net carbon fixation from kinetic fluorescence analysis

Comparisons of amplitude-based variable fluorescence and ^{14}C measurements of primary production in diverse biogeochemical regions of the ocean revealed that the electron requirements for carbon fixation are influenced by the extent of nutrient limitation and also may vary with taxonomy and

other factors (Lawrenz et al. 2013; Zhu et al. 2017; Hughes et al. 2018*b*). Closer examination of environmental factors that may control the electron requirements suggests that nutrient and, more specifically, nitrogen limitation imposes a major control (Hughes et al. 2018*b*; Ko et al. 2019). Our results corroborate these field observations and provide a mechanistic understanding and quantitative characterization of the impact of nitrogen limitation on the growth rates and the electron yields of net carbon fixation. The electron yield for net primary production is maximal under nitrogen-replete conditions and decreases down to near-zero under severe nitrogen starvation (Fig. 6). The application of fluorescence kinetic analysis allowed us to develop a simple fluorescence-based indicator to predict the electron yields of carbon fixation for the conditions of nitrogen limited growth.

Our examination revealed a linear correlation between instantaneous growth rates and the kinetic-based measurements of photosynthetic turnover rates (Figs. 4C, 5C) under nitrogen-limited growth. This result clearly suggests that the electron yield of net carbon production for nitrogen-limited growth is controlled by and can be estimated from a relative reduction in photosynthetic turnover rates (Eq. 16).

We propose a simple algorithm to deduce the electron yield of net carbon production, Φ_{NPc} (Eq. 16) from the ratio $x = \tau_{replete}/\tau$, based on fluorescence kinetic measurements. The turnover rate $\tau_{replete}$ for nutrient-replete plankton is critical for calculating the x ratio and for this algorithm. The absolute value of τ alone is not sufficient for quantifying the extent of nitrogen limitation. Beside nitrogen limitation, the absolute values of τ are strongly affected by other environmental factors, such as photo-acclimation and temperature. For instance, our experiments showed that low-light acclimation decreases $1/\tau$ two to three times, as compared its value under high light. Low temperature also decreases dramatically the turnover rates. For example, $1/\tau$ is five to eight times lower in nutrient-replete Arctic waters, as compared to sub-tropical regions of the ocean. Severe nitrogen limitation in the Arctic ocean in the summer further decreases $1/\tau$ by a factor of ca. two, suggesting dramatic reduction in growth rates and net primary production (Ko et al. 2019). While field sampling, the turnover rate for nitrogen-replete plankton ($1/\tau_{replete}$) and the ratio $x = \tau_{replete}/\tau$ can be readily measured using a short-term ($\sim$ 24 h) nutrient enrichment incubations, which alleviate nutrient stress and thus recover $1/\tau_{replete}$.

In marine ecosystems, photosynthetic rates have traditionally been measured by following the uptake of radioactive inorganic carbon into particulate organic matter. The ^{14}C uptake method, pioneered by (Steemann Nielsen 1952) is extremely sensitive, but requires an incubation of samples in a confined space. By the late 1970s, it became increasingly clear that incubation of samples in bottles, especially in the oligotrophic open ocean, could lead to large artifacts due to trace metal contamination (Carpenter and Lively 1980; Fitzwater et al. 1982), and from alterations in the community structure during longer-term incubations (Eppley 1980). The measured rates of ^{14}C uptake depend dramatically on the incubation duration (Marra 2009; Halsey et al. 2011, 2013). Also, the results of short-term ^{14}C incubations strongly depend on the extent of nitrogen limitation (Halsey et al. 2011, 2013), reflecting gross production rates in nutrient replete phytoplankton and net production rates in nitrogen limited plankton. This difference between gross and net production rates is > 100%, thus introducing large errors to the interpretation of short-term ^{14}C incubations, if the extent of nutrient stress is not a priori known (Halsey et al. 2011; Milligan et al. 2015). Our developed fluorescence kinetic analysis offers an easily measured quantitative index of nutrient stress, in relation to growth rates. This index is critically needed for accurate interpretation of ^{14}C uptake measurements when the extent of nutrient stress varies.

References

Carpenter, E. J., and J. S. Lively. 1980. Review of estimates of algal growth using ^{14}C tracer techniques, p. 161–178. *In* P. G. Falkowski [ed.], Primary productivity in the sea. Plenum Press.

Crofts, A. R., and C. A. Wraight. 1983. The electrochemical domain of photosynthesis. Biochim. Biophys. Acta **726**: 149–185. doi:10.1016/0304-4173(83)90004-6

Dugdale, R. C. 1967. Nutrient limitation in the sea: Dynamics, identification, and significance. Limnol. Oceanogr. **12**: 685–695. doi:10.4319/lo.1967.12.4.0685

Eppley, R. W. 1980. Estimating phytoplankton growth rates in the central oligotrophic oceans, p. 231–242. *In* P. G. Falkowski [ed.], Primary productivity in the sea. Plenum Press.

Falkowski, P. G., K. Wyman, A. C. Ley, and D. C. Mauzerall. 1986. Relationship of steady state photosynthesis to fluorescence in eukaryotic algae. Biochim. Biophys. Acta **849**: 183–192. doi:10.1016/0005-2728(86)90024-1

Falkowski, P. G., and Z. Kolber. 1995. Variations in the chlorophyll fluorescence yields in the phytoplankton in the world oceans. Aust. J. Plant Physiol. **22**: 341–355. doi:10.1071/PP9950341

Falkowski, P. G., M. Koblizek, M. Gorbunov, and Z. Kolber. 2004. Development and application of variable chlorophyll fluorescence techniques in marine ecosystems, p. 757–778. *In* G. C. Papageorgiou and Govingjee [eds.], Chlorophyll a fluorescence: A signature of photosynthesis. Springer.

Falkowski, P. G., and J. A. Raven. 2014. Aquatic photosynthesis, 2nd ed. Princeton Univ. Press.

Fitzwater, S. E., G. A. Knauer, and J. H. Martin. 1982. Metal contamination and its effects on primary production measurements. Limnol. Oceanogr. **27**: 544–551. doi:10.4319/lo.1982.27.3.0544

Genty, B., J. M. Briantais, and N. R. Baker. 1989. The relationship between the quantum yield of photosynthetic electron

transport and quenching of chlorophyll fluorescence. Biochim. Biophys. Acta **990**: 87–92. doi:10.1016/S0304-4165(89)80016-9

Genty, B., J. Harbinson, J. M. Briantais, and N. R. Baker. 1990. The relationship between non-photochemical quenching of chlorophyll fluorescence and the rate of photosystem-2 photochemistry in leaves. Photosynth. Res. **25**: 249–257. doi:10.1007/BF00033166

Gorbunov, M. Y., Z. S. Kolber, and P. G. Falkowski. 1999. Measuring photosynthetic parameters in individual algal cells by fast repetition rate fluorometry. Photosynth. Res. **62**: 141–153. doi:10.1023/A:1006360005033

Gorbunov, M. Y., P. G. Falkowski, and Z. S. Kolber. 2000. Measurement of photosynthetic parameters in benthic organisms in situ using a SCUBA-based fast repetition rate fluorometer. Limnol. Oceanogr. **45**: 242–245. doi:10.4319/lo.2000.45.1.0242

Gorbunov, M. Y., Z. S. Kolber, M. P. Lesser, and P. G. Falkowski. 2001. Photosynthesis and photoprotection in symbiotic corals. Limnol. Oceanogr. **46**: 75–85. doi:10.4319/lo.2001.46.1.0075

Gorbunov, M. Y., and P. G. Falkowski. 2005. Fluorescence induction and relaxation (FIRe) technique and instrumentation for monitoring photosynthetic processes and primary production in aquatic ecosystems. Photosynthesis: Fundamental aspects to global perspectives, p. 1029–1031. *In* 13th international congress of photosynthesis. V. 2.

Gorbunov, M. Y., E. Shirsin, E. Nikonova, V. V. Fadeev, and P. G. Falkowski. 2020. The use of multi-spectral fluorescence induction and relaxation technique for physiological and taxonomic analysis of phytoplankton communities. Mar. Ecol. Prog. Ser. **644**: 1–13. doi:10.3354/meps13358

Halsey, K. H., A. J. Milligan, and M. J. Behrenfeld. 2011. Linking time-dependent carbon-fixation efficiencies in *Dunaliella tertiolecta* (chlorophyceae) to underlying metabolic pathways. J. Phycol. **47**: 66–76. doi:10.1111/j.1529-8817.2010.00945.x

Halsey, K. H., R. T. O'Malley, J. R. Graff, A. J. Milligan, and M. J. Behrenfeld. 2013. A common partitioning strategy for photosynthetic products in evolutionarily distinct phytoplankton species. New Phytol. **198**: 1030–1038. doi:10.1111/nph.12209

Halsey, K. H., A. J. Milligan, and M. J. Behrenfeld. 2014. Contrasting strategies of photosynthetic energy utilization drive lifestyle strategies in ecologically important picoeukaryotes. Metabolites **4**: 260–280. doi:10.3390/metabo4020260

Herron, H. A., and D. Mauzerall. 1971. The development of photosynthesis in a greening mutant of chlorella and an analysis of the light saturation curve. Plant Physiol. **50**: 141–148. doi:10.1104/pp.50.1.141

Hughes, D. J., and others. 2018*a*. Roadmaps and detours: Active chlorophyll-a assessments of primary productivity across marine and freshwater systems. Environ. Sci. Technol. **52**: 12039–12054. doi:10.1021/acs.est.8b03488

Hughes, D. J., D. Varkey, M. A. Doblin, T. Ingleton, A. Mcinnes, P. J. Ralph, V. van Dongen-Vogels, and D. J. Suggett. 2018*b*. Impact of nitrogen availability upon the electron requirement for carbon fixation in Australian coastal phytoplankton communities. Limnol. Oceanogr. **63**: 1891–1910. doi:10.1002/lno.10814

Juranek, L. W., and P. D. Quay. 2013, 2013. Using triple isotopes of dissolved oxygen to evaluate global marine productivity Annu. Rev. Mar. Sci. **5**: 503–524. doi:10.1146/annurevmarine-121211-172430

Ko, E., J. Park, M. Y. Gorbunov, and S. Yoo. 2019. Uncertainties in variable fluorescence and 14C methods to estimate primary productivity: A case study in the coastal waters off the Korean peninsula. Mar. Ecol. Prog. Ser. **627**: 13–31. doi:10.3354/meps13083

Kolber, Z., J. Zehr, and P. G. Falkowski. 1988. Effects of growth irradiance and nitrogen limitation on photosynthetic energy conversion in photosystem II. Plant Physiol. **88**: 923–929. doi:10.1104/pp.88.3.923

Kolber, Z., and P. G. Falkowski. 1993. Use of active fluorescence to estimate phytoplankton photosynthesis in-situ. Limnol. Oceanogr. **38**: 1646–1665. doi:10.4319/lo.1993.38.8.1646

Kolber, Z., O. Prasil, and P. G. Falkowski. 1998. Measurements of variable chlorophyll fluorescence using fast repetition rate techniques: Defining methodology and experimental protocols. Biochim. Biophys. Acta **1367**: 88–106. doi:10.1016/S0005-2728(98)00135-2

Lawrenz, E., and others. 2013. Predicting the electron requirement for carbon fixation in seas and oceans. PLOS One **8**: e58137. doi:10.1371/journal.pone.0058137

Levitan, O., J. Dinamarca, E. Zelzion, M. Y. Gorbunov, and P. G. Falkowski. 2015. An RNAi knock-down of nitrate reductase enhances lipid biosynthesis in the diatom *Phaeodactylum tricornutum*. Plant J. **84**: 963–973. doi:10.1111/tpj.13052

Lin, H., F. I. Kuzminov, J. Park, S. H. Lee, P. G. Falkowski, and M. Y. Gorbunov. 2016. The fate of photons absorbed by phytoplankton in the global ocean. Science **351**: 264–267. doi:10.1126/science.aab2213

Litchman, E., and C. A. Klausmeier. 2008. Trait-based community ecology of phytoplankton. Annu. Rev. Ecol. Evol. Syst. **39**: 615–639. doi:10.1146/annurev.ecolsys.39.110707.173549

Marra, J. 2009. Net and gross productivity: Weighing in with ^{14}C. Aquat. Microb. Ecol. **56**: 123–131. doi:10.3354/ame01306

McElroy, M. B. 1983. Marine biological controls on atmospheric CO_2 and climate. Nature **302**: 328–329. doi:10.1038/302328a0

Milligan, A. J., K. H. Halsey, and M. J. Behrenfeld. 2015. Advancing interpretations of ^{14}C-uptake measurements in the context of phytoplankton physiology and ecology. J. Plankton Res. **37**: 692–698. doi:10.1093/plankt/fbv051

Moore, C. M., and others. 2013. Processes and patterns of oceanic nutrient limitation. Nat. Geosci. **6**: 701–710. doi:10.1038/ngeo1765

Myers, J., and J. R. Graham. 1971. The photosynthetic unit of Chlorella measured by repetitive short flashes. Plant Physiol. **48**: 282–286. doi:10.1104/pp.48.3.282

Oxborough, K., C. M. Moore, D. J. Suggett, T. Lawson, H. G. Chan, and R. J. Geider. 2012. Direct estimation of functional PSII reaction center concentration and PSII electron flux on a volume basis: A new approach to the analysis of Fast Repetition Rate fluorometry (FRRf) data. Limnol. Oceanogr.: Methods **10**: 142–154. doi:10.4319/lom.2012.10.142

Parkhill, J.-P., G. Maillet, and J. J. Cullen. 2001. Fluorescence-based maximal quantum yield for PSII as a diagnostic of nutrient stress. J. Phycol. **37**: 517–529. doi:10.1046/j.1529-8817.2001.037004517.x

Schuback, N., C. J. Hoppe, J. É. Tremblay, M. T. Maldonado, and P. D. Tortell. 2017. Primary productivity and the coupling of photosynthetic electron transport and carbon fixation in the Arctic Ocean. Limnol. Oceanogr. **62**: 898–921. doi:10.1002/lno.10475

Steemann Nielsen, E. 1952. The use of radio-active carbon (C14) for measuring organic production in the sea. ICES J. Mar. Sci. **18**: 117–140. doi:10.1093/icesjms/18.2.117

Sunda, W. G., and S. A. Huntsman. 1997. Interrelated influence of iron, light and cell size on marine phytoplankton growth. Nature **390**: 389–392. doi:10.1038/37093

Zhu, Y., J. Ishizaka, S. C. Tripathy, S. Wang, C. Sukigara, J. Goes, T. Matsuno, and D. J. Suggett. 2017. Relationship between light, community composition and the electron requirement for carbon fixation in natural phytoplankton. Mar. Ecol. Prog. Ser. **580**: 83–100. doi:10.3354/meps12310

Acknowledgments

This research was supported by NASA Ocean Biology and Biogeochemistry Program (Grants NNX16AT54G and 80NSSC18K1416). We thank Jonathan Sherman, Eunho Ko, and Jisoo Park for assistance with field data collection, Kevin Wyman for suggestions on the manuscript, and anonymous reviewers and the editor for constructive comments.

Conflict of Interest

None declared.

Submitted 23 June 2020
Revised 23 July 2020
Accepted 28 July 2020

Associate editor: Susanne Menden-Deuer